On Particulate Matter and Direct Irradiation as Confounding Factors on the Prediction of Viruses Viability and Spread: the Meaningful Case of the SARS-CoV-2 Diffusion in Italy

Angelo Spena[1], *Francesco* Biso[1*], and *Vincenzo Andrea* Spena[2]

[1]Department of Enterprise Engineering, Tor Vergata University of Rome, Italy
[2]Department of Aeronautical, Electrical and Energy Engineering, Sapienza University of Rome, Italy

Abstract. Climate change and air pollutants are increasingly stressing our environment; among other consequences, this increases the need for deeper insights into how epidemiological patterns respond to these factors, as dramatically shown in recent years. Parameters such as temperature and humidity have been identified as the main drivers of both indoor and outdoor viruses viability. In this context, the present paper proposes a general framework to define and quantify two corrective coefficients capturing the combined effects of particulate matter and solar ultraviolet radiation levels as confounding factors in virus diffusion detection. This is particularly relevant within the framework of the Enthalpy Method, an approach introduced in 2020 for pandemic risk assessments based on the combined values of inner temperature and humidity. The presented results, based on the case of SARS-CoV-2 in Italy – a recognized unique setting in terms of data extent, reliability, and climatic range – indicate that air pollution levels alone played a major role in fine-tuning Incidence Rate (IR) predictions, while sunlight was also found to significantly improve IR predictions, although to a lesser extent than PM_{10} when considered individually. The inferred interaction between the two correction coefficients is examined from a comprehensive perspective, leading to suggestions for tailored evaluations in different contexts.

1 Introduction

Climate change and air pollutants are increasingly stressing our environment; this enhances the need for deeper insights into the epidemiological sensitivities to those factors. In this study, we provide an extension of the Enthalpy Method, which we have previously introduced in the risk assessment literature to predict virus survival, as well as the Incidence Rate of the COVID-19 pandemic. As extensively discussed in the literature for decades by authors such as de Jong, Winkler, Hemmes and Ijaz, temperature and humidity play a crucial role in the survival of a number of viruses, i.e. SARS-CoV, MERS-CoV and influenza, to which SARS-CoV-2 has recently been added [1]. However, despite an increasing but

* Francesco Biso: francesco.biso@uniroma2.it

inconclusive number of studies claiming for geographic and climatic possible influence on SARS-CoV-2 outbreak and spread, in one of our previous works [2] it was stressed that neither temperature nor humidity could be correlated independently with the virus viability. Yet, since human coronaviruses have been shown to display a strong winter seasonality – despite some authors such as Cappi disputing a recurrent seasonal pattern – the specific enthalpy of atmospheric air at ground level may be used as a synthetic parameter to evaluate the synergic primary role of both temperature and humidity. As a result, a strong relationship between the virus survival and the specific outdoor and indoor enthalpy of moist air seems emerged [2,3]. As far as the possibility that secondary weather conditions can play an independent role in the COVID-19 onset and transmission is concerned [4], several other related factors must be compounded in scenarios not only of high complexity but also dominated by wide uncertainties [5]. As previously stated [3], on the total population the available number of cases, and especially of deaths, are also influenced at least by: i) the number of investigations carried out, their statistic assessment and possible underestimations [6]; ii) demography, as population age and density [7]; iii) urban layout, mobility and indoor social habits of a population [8]; iv) hospital settings, medical care and susceptibility of the hosts [9]. All factors almost unrelated to the specific enthalpy.

Here, the role of particulate matter pollution PM and of UV radiation as potential co-factors responsible for the magnification or reduction of SARS-CoV-2 infectivity and diffusion will be explored, especially in the Enthalpy Method framework. This study aims to demonstrate that removing the estimated contribution of environmental factors such as particulate matter and sunlight enhances the accuracy with which models can predict the outdoor and indoor spread of an infection. Through a case study on the diffusion of COVID-19 in Italy in the early year 2020, a formulation for corrective coefficients will be proposed based on the available data, demonstrating that the precision of the Enthalpy Method in predicting the Incidence Rate (IR) can be further improved.

2 Materials and Methods

2.1 Enthalpy Method Rationale

The present work is based on the *Enthalpy Method*, since 2020 proposed [2] and successfully adopted [3,10], to provide an effective synthetic representation of the thermo-hygrometric state of atmospheric moist air at ground level in terms of both air temperature and RH through its specific enthalpy value *h*, which facilitates correlation between environmental conditions and the COVID-19 Incidence Rate (IR), calculated as the ratio between the number of ascertained cases and the total population [3]. In the present work, the specific enthalpy will be used assuming, as usual, h=0 at zero water content (dry air) and zero degrees centigrade, and calculated as follows:

$$h = c_a \cdot t + AH \cdot (c_v \cdot t + r) \qquad (1)$$

where c_a and c_v are the specific heats at the constant pressure of dry air and of water vapour, which, around ambient temperature, can be assumed as equal to 1.006 $kJ \cdot kg^{-1} \cdot °C^{-1}$ and 1.86 $kJ \cdot kg^{-1} \cdot °C^{-1}$, respectively, AH is the absolute humidity of moist air AH in $kg_v \cdot kg_{dry\text{-}air}^{-1}$, t is the air temperature in degrees centigrade, and r is the latent heat of vaporisation of water at its triple point, equal to 2501 $kJ \cdot kg^{-1}$.

2.2 Environmental Data

For the present work, environmental data for 30 Italian provinces were gathered (see Table 1 in §3.1). As a source of air pollution measurements, in order to rely on data of high quality, only the data made available by the official Italian regional environmental agencies (ARPA, ARTA, APPA) were used. Data on PM2.5 were not always available; for that reason, it was decided to use the PM_{10} records that were normally available for almost all the provinces studied. The following sources were accessed (last access May 2024): ARTA Abruzzo for L'Aquila and Teramo; ARPA Basilicata for Potenza; ARPA Campania for Napoli; ARPA Calabria for Reggio Calabria; ARPA Emilia-Romagna for Parma and Piacenza; ARPA FVG for Trieste; ARPA Lazio for Roma and Latina; ARPA Liguria for Genova and Savona; ARPA Lombardia for Bergamo, Brescia, Cremona, Lodi and Milano; ARPA Marche for Pesaro; Arpa Piemonte for Alessandria and Torino; ARPA Puglia for Bari and Brindisi; ARPA Sardegna for Cagliari; ARPA Sicilia for Palermo; ARPA Toscana for Firenze; APPA Trento for Trento; ARPA Umbria for Perugia; ARPA Valle d'Aosta for Aosta; ARPA Veneto for Verona. The air pollution data (urban area) of the capital of provinces were considered as representative of the whole area, by reason of the fact that the capitals are the most populated cities of the area and so the majority of the population is exposed to that level of air pollution. The data made available by the Joint Research Centre of the European Commission via the Photovoltaic Geographical Information System (PVGIS), based on data from satellites and reanalysis, were employed as a source for Direct Irradiation (DI) estimates. The SARAH3 solar radiation data for every hour of the direct beam irradiation on a plane always normal to sun rays were chosen, and the 10-day average value for each city was calculated. The values are reported in Table 2 in §3.2.

2.3 Particulate Matter Correction

Correlations between the number of infected people and atmospheric particulate levels like $PM_{2.5}$ and PM_{10} are still controversial, as the particulate acts twice: i) as a carrier, increasing the virus transport; and ii) as a booster making the virus find host's respiratory health conditions already compromised [11–13]. In order to evaluate whether the particulate matter may or may not significantly modify the Incidence Rate IR, and referring again to the decade falling from 20 to 30 days before the first death, the analysis of the possible effects of PM_{10} here assumed as reference for the sake of generality will be conducted as follows by correcting the value of IR using a PM-related multiplying factor f_{PM} defined as:

$$f_{PM} = \min\{1, (\mathrm{T_{PM10}}/C_{PM10})^{a}\} \quad (2)$$

where T_{PM10}=50 μg·m^{-3} is the PM_{10} daily threshold officially imposed until 2026 by Directive (EU) 2024/2881 of the European Parliament and Council of 23 October 2024, which was assumed as a reference; and C_{PM10} is the average PM_{10} concentration recorded in any considered city during the 10-day observation period. The exponent a will be further defined in §3.1 based on targeted preliminary evaluations. Now, with the PM correction factor f_{PM} as defined in Equation (2), it is possible to calculate a corrected IR as follows:

$$IR_{PM} = f_{PM} \cdot IR \quad (3)$$

where IR is the IR basically calculated from the pandemic data, and IR_{PM} is the Incidence Rate corrected for the effect of the particulate matter. Notice that, according to Equation 2, in all those cases in which the concentration of PM_{10} is lower than the threshold, the value of IR is maintained unaltered as if the effect of particulate matter as a potential carrier of the

virus were negligible. Conversely, in case of concentrations of PM_{10} higher than the threshold, the fraction of the Incidence Rate due to the mere specific enthalpy of atmospheric air has been reduced using the correction factor f_{PM} in order to account for the potential additional contribution of the particulate matter to the COVID-19 diffusion.

2.4 Ultraviolet Radiation Correction

Similarly, to explore whether the possible influence of sunlight and especially of UV radiation [14] may or may not modify the results obtainable with the proposed method, in Equation (4) the UV correction factor f_{UV} is defined, to some extent accounting for possible outdoor virus inhibition effects due to the UV light, and here assumed as:

$$f_{UV} = \min\{1, (DI/DI_{mean})^{b}\} \quad (4)$$

where, for the sake of practicability, overall beam irradiation is assumed, in terms of relative levels comparisons, as a proxy of the ultraviolet radiation. Thus, f_{UV} is the ratio between the 10-day observation period average value for the specific city of the daily value of the overall Direct (beam) Irradiation DI [$kWh \cdot m^{-2} \cdot day^{-1}$], and DI_{mean} is the mean level of daily direct irradiation over the cities considered. Again, the exponent b will be further defined in §3.1 based on targeted preliminary evaluations. If the former falls above the DI_{mean} value, the ratio is still equal to 1 (again, a sort of non-recognition of the influence of the UV on the SARS-CoV-2 virulence). Similarly to the PM effect introduced in §2.3, with the UV correction factor f_{UV} as previously formulated, a corrected IR can be calculated as follows:

$$IR_{UV} = f_{UV} \cdot IR \quad (5)$$

where IR is the IR calculated from the pandemic data, and IR_{UV} is the Incidence Rate corrected for the effect of ultraviolet radiation.

2.5 Interaction Between PM and UV Effects

The two environmental agents can interact in the same period of time, so it would be natural to define the corrected synergic IR as follows:

$$IR_{COR} = f_{PM} \cdot f_{UV} \cdot IR = f_{COR} \cdot IR. \quad (6)$$

Each one of the two environmental agents considered, namely particulate matter and ultraviolet radiation, can be thought to affect both the viability or the ability to spread of the virus and the host. On the host side, PM_{10} can affect the respiratory tract, resulting in inflammation and increased susceptibility to infections [15], while UV radiation is responsible for the synthesis of Vitamin D and is relevant for the immune system. Additionally, since the two corrections act accordingly and the PM_{10} concentration in the atmosphere contributes to its UV absorption, it was decided to account for a synergy of the factors on the host side defined in §2.3 and 2.4 as follows:

$$\text{if } (f_{PM} < 1 \text{ AND } f_{UV} < 1) : f_{COR} = {f_{PM}}^{0.75} \cdot {f_{UV}}^{0.75} \quad (7a)$$
$$\text{else: } f_{COR} = f_{PM} \cdot f_{UV}. \quad (7b)$$

3 Results

3.1 Procedure Assessment

For the present study, the IR was calculated in the first 40 days after the first reported case of SARS-CoV-2 virus in 2020 in 30 Italian provinces, i.e. before substantial medical or behavioural public interventions acting as a non-climatic confounding factor [3]. For any province, the h value was more accurately evaluated by considering the time evolutions of air temperature and of AH during the 20–30 days prior to the first reported case [3]. Since the weather data were available from airport weather stations rather than urban weather stations, a reasonably average 1.5 °C increase was applied to the temperature data before calculating h in order to account for the well-known urban heat island (UHI) effect, as well as the notion that, in winter, the UHI effect is generally less pronounced than in summer as can be understood by the works of authors such as Santamouris. Thus, instead of using the 10-day average temperature and humidity values to calculate the average h, the 10-day average h of the atmospheric air was obtained as the median of the ten daily average h values, each determined by replacing the daily average temperature and AH [3]. The results are listed in Table 1. The proposed set of Italian provinces, which can be considered a representative sample of the whole country since approximately at least 42% of the Italian people live there, is undoubtedly homogeneous in terms of social habits; additionally, the climatic conditions of Italy span from those typical of the high-altitude mountains of Northern Italy (up to 46.5 °N latitude) to those of the Mediterranean coastal areas (down to 36.5 °N latitude). All the above usefully allowed us to explore a significantly wide range of both IR (0.02 to 1.18) and h (9.6 to 37.6 kJ/kg) values.

Table 1. Data of the selected 30 Italian provinces [3].

Provinces	ID#	Population	Cases after 40 days	IR [%]	h [kJ·kg^{-1}]
Alessandria	1	421,284	2248	0.53	23.6
Aosta	2	125,666	993	0.79	16.0
Bari	3	1,251,994	886	0.07	27.0
Bergamo	4	1,114,590	9712	0.87	18.9
Brescia	5	1,265,954	9477	0.75	21.8
Brindisi	6	392,975	428	0.11	28.6
Cagliari	7	431,038	191	0.04	33.3
Campobasso	8	221,238	191	0.09	9.6
Cremona	9	358,955	4233	1.18	15.9
Firenze	10	1,011,349	1715	0.17	32.2
Genova	11	841,180	2918	0.35	30.6
L'Aquila	12	299,031	220	0.07	9.6
Latina	13	575,254	419	0.07	26.2
Lodi	14	230,198	2255	0.98	20.2
Milano	15	1390434	10149	0.73	19.1
Napoli	16	3,084,890	1643	0.05	29.3
Palermo	17	1,252,588	299	0.02	37.6
Parma	18	451,631	2083	0.46	25.9
Perugia	19	656,382	950	0.14	26.2

Pesaro	20	358,886	1919	0.53	23.2
Piacenza	21	287,152	2892	0.79	19.6
Potenza	22	364,960	162	0.07	28.3
Reggio Calabria	23	548,009	276	0.87	28.1
Roma	24	4,342,212	2714	0.75	32.0
Savona	25	276,064	654	0.11	27.8
Teramo	26	308,052	511	0.04	26.4
Torino	27	2,256,523	5985	0.09	20.6
Trento	28	541,098	3053	1.18	11.8
Trieste	29	234,493	821	0.17	24.8
Verona	30	962,497	3049	0.35	25.0

As a first step, data visualisation was used to understand if outliers were present in our dataset (Fig. 1). While exploring, it was noted that the province of Torino, after the correction, shifted towards the bottom of the plot with an unexpected behaviour. Searching for information about the correctness of the IR data registered for this province it was discovered that, when the pandemic was starting, there was a lack of SARS-CoV-2 tests to check the patients. For these reasons, it was decided to mark Torino as an outlier and to remove the province of Torino from the dataset. In a previous paper, it was demonstrated that [3] the IR is correlated with the specific enthalpy of the environmental air of the area under consideration. In order to understand and measure if PM or UV affect the IR prediction based on the specific enthalpy, it was decided to fit the model for those provinces in our dataset which have the correction factor (f_{PM} or f_{UV} respectively) equal to 1 and are, therefore, supposed not affected by the environmental condition under consideration. This decision allowed the definition of baseline models, neutral to PM and UV effect (Fig. 2), for the calculation of the expected IR based on the enthalpy of the area considered. To do this, an interpolation equation was fitted on the subset of provinces, coherent with that successfully used [3] for the Enthalpy Method validation, which, coherently with the previous findings, shows the peak present for a specific enthalpy in the range from 12 to 23 kJ·kg^{-1} [3]:

$$IR(\%) = \mathrm{e}^{49.671} \cdot h^{-13.303} \cdot \left(\mathrm{e}^{210.238/h} - 1\right)^{-1}. \quad (8)$$

It is worth noting, as shown in Fig. 2 – upper left panel, a lack of points in the range of specific enthalpy from 11.8 (Trento) to 23.2 (Pesaro) kJ·kg^{-1}. This incidental data shortage could cause the calculation results to lack reliability and robustness. Yet the definition of a neutral model was further investigated on two (different) subsets, either neutral to PM or UV independently (See Fig. 2 – upper right and lower left panel). In Fig. 2 – upper right panel is presented the baseline interpolation for the Italian provinces within our dataset that do not need a correction for the air quality (namely, the mean concentration of PM_{10} does not exceed the limit of 50 μg·m^{-3}) based on the definition of the factor f_{PM}:

$$IR(\%) = \mathrm{e}^{45.529} \cdot h^{-12.187} \cdot \left(e^{194.223/h} - 1\right)^{-1}. \quad (9)$$

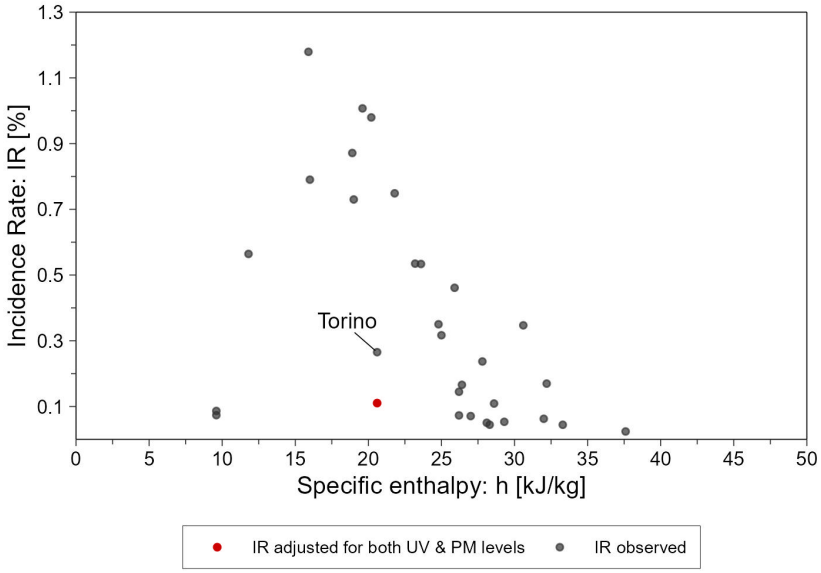

Fig. 1. Scatterplot of Incidence Rate (IR) vs specific enthalpy (h) for the Italian provinces with the highlight of Torino, which appears to be an outlier. Observed IR (black); predicted IR after the corrections proposed, namely f_{PM} and f_{UV} (red).

The fitting is coherent with the previous findings showing that the peak is still present for a specific enthalpy around an enthalpy of 15 kJ·kg^{-1}; moreover, in this subset, the province of Aosta with an enthalpy of 16 kJ·kg^{-1} is included. In Fig. 2 – lower left panel, the baseline interpolation for the Italian provinces within our dataset that do not need a correction for the UV radiation, namely the mean DI irradiation of a city over the average DI irradiation (calculated over all the cities) based on the definition of the factor f_{UV}, is presented:

$$IR(\%) = e^{54.646} \cdot h^{-14.546} \cdot \left(e^{231.740/h} - 1\right)^{-1}. \quad (10)$$

It should be noted that this subset faces again a lack of data in the range between 15.9 to 23.6 kJ·kg^{-1}. A comparison of the three fits (see Fig. 2 – lower right panel) shows that the fit neutral to both PM and UV is close to both the UV-neutral and PM-neutral fits, although the subset neutral to both factors (PM and UV) contains sparse data around the IR peak. Moreover, the UV-neutral fit appears to underestimate the observed peak, (again) likely because the UV-neutral subset contains few data points in the IR peak region, while still locating the IR maximum correctly.

Based on the comparison, the PM-neutral fitting was selected as representative of the data not affected by pollution and radiation interferences with the typical virus spread.

Once the reference model was defined, the exponents a and b of Equations (2) and (4) were independently determined through an iterative process aimed at minimizing the model error, assessed via the root mean square error (RMSE). This optimization was conducted within the range of 0.5–3.0 with a step size of 0.1, assuming that the corrective factors could be a radical, linear, quadratic, or at most cubic function of the ratios of the significant quantities defined in Equations (2) and (4). The RMSE-based optimization, using air quality data, identified an optimal exponent for the corrective factor f_{PM} of around 1.8. Conversely, for the corrective factor f_{UV}, the optimal exponent was found to be around 1.5. Fig. 3 illustrates the variation of RMSE as a function of the exponents a and b under investigation.

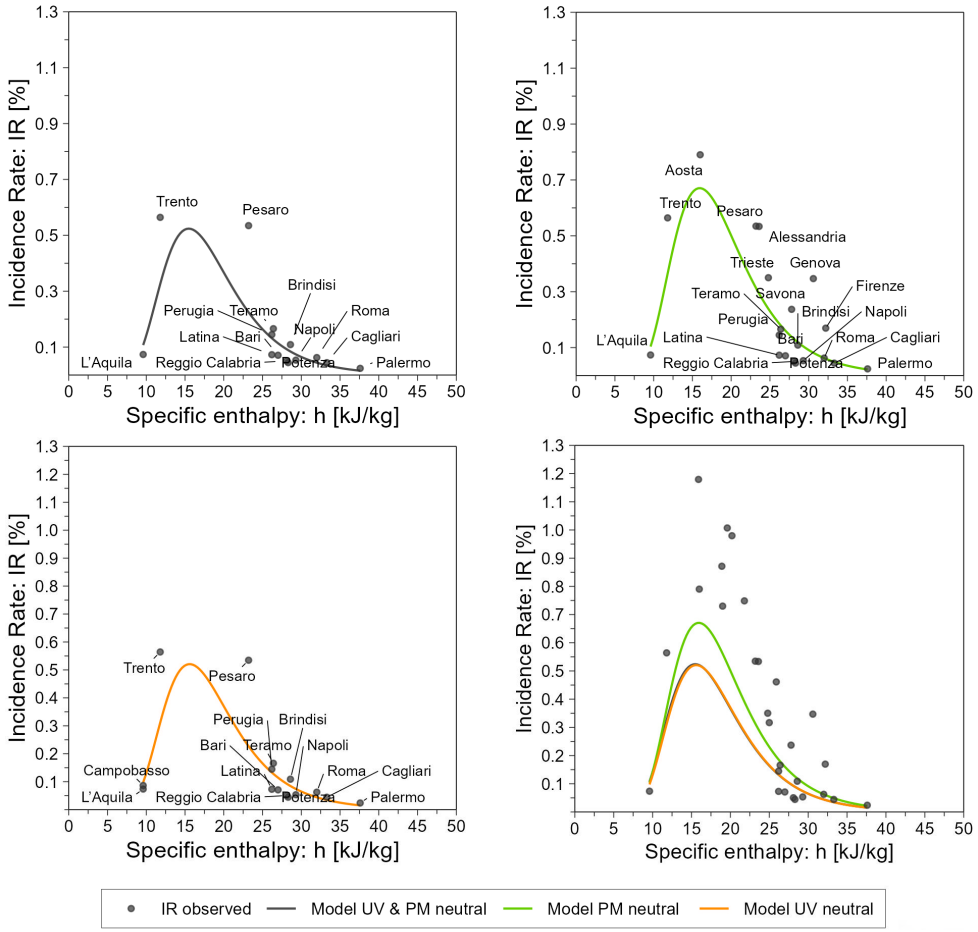

Fig. 2. Interpolation curve Incidence Rate (IR) vs. specific enthalpy (h) for the provinces: upper left) not affected by PM and UV corrections as defined in §2.3, 2.4 and 2.5; upper right) not affected by PM correction as defined in §2.3; lower left) not affected by UV correction as defined in §2.4; lower right) for the three neutral subsets (black: both; green: PM; orange: UV).

It can be observed (Fig. 3) that the curve corresponding to exponent a for f_{PM} exhibits a minimum (1.8) positioned at the centre of a saddle-shaped region between 1.4 and 2.2. This suggests a markedly nonlinear dependence of the corrective factor on the ratio of the reference quantities. Conversely, the curve corresponding to exponent b for f_{UV} presents a minimum (1.5) centered within a saddle-shaped region spanning from 0.8 to 2.0. Moreover, the iterative process was conducted on data inherently affected by noise due to additional confounding factors, which inevitably influence the results. In addition, each time one of the two environmental factors considered (PM or UV) is under consideration, it remains interlinked with the interference of the other environmental factor. Given that the minimum and the optimal region for PM_{10} appear more distinct and clearly exceeding the linearity, a conservative choice seemed to adopt an exponent b of 1.5. In the case of the corrective factor f_{UV}, the optimal region appears shifted towards lower values of exponent b, while on the right-hand side of the curve the error increases rapidly. For this reason, a conservative value of 1.0 was chosen, as a linear dependence aligns with the observed saddle region. All above lead to:

$$f_{PM} = \min\{1, (\mathrm{T_{PM10}}/C_{PM10})^{1.5}\}, \mathrm{f_{UV}} = \min\{1, (DI/DI_{mean})^{1}\} \qquad (11)$$

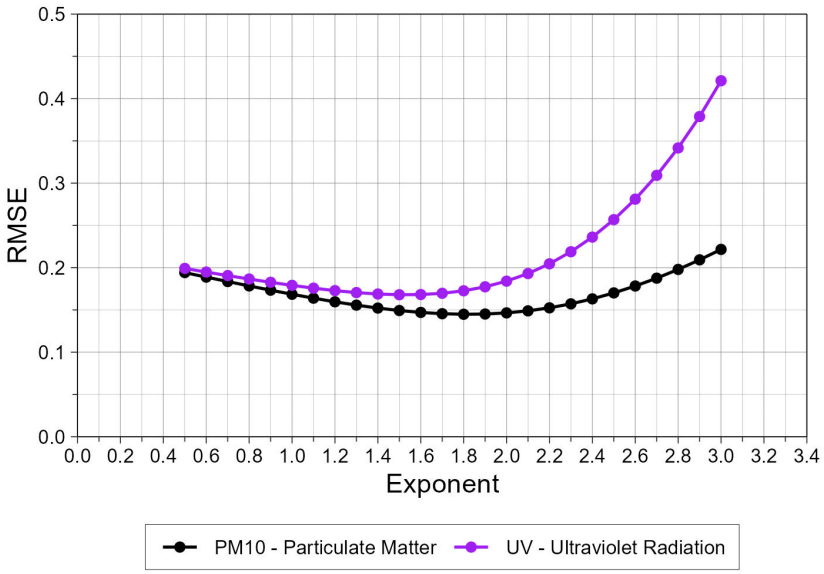

Fig. 3. RMSE as a function of the exponents a and b of the f_{PM} and f_{UV} corrective factors, respectively; (black: RMSE as a function of exponent a; purple: RMSE as a function of the exponent b).

3.2 Particulate Matter Effect on Incidence Rate

The results of the calculations for the f_{PM} factor (as defined in §2.3) and the data required are listed in the following Table 2.

Table 2. Italian provinces (30) dataset for the PM_{10} and UV effects corrections.

ID#	PM_{10} level [µg·m^{-3}]	PM_{10} EU-limit [µg·m^{-3}]	f_{PM}	DI level [kWh·m^{-2}]	DI_{mean} [kWh·m^{-2}]	f_{UV}
1	41.85	50.0	1.000	3.89	3.51	1.000
2	20.66	50.0	1.000	2.77	3.51	0.789
3	25.13	50.0	1.000	4.03	3.51	1.000
4	59.10	50.0	0.778	3.74	3.51	1.000
5	61.20	50.0	0.738	3.16	3.51	0.901
6	18.40	50.0	1.000	4.33	3.51	1.000
7	31.33	50.0	1.000	4.66	3.51	1.000
8	na	50.0	na	3.82	3.51	1.000
9	66.10	50.0	0.658	2.59	3.51	0.738
10	23.73	50.0	1.000	1.08	3.51	0.306
11	19.41	50.0	1.000	2.53	3.51	0.721
12	15.13	50.0	1.000	3.77	3.51	1.000
13	29.39	50.0	1.000	4.59	3.51	1.000
14	66.35	50.0	0.654	2.53	3.51	0.719
15	72.25	50.0	0.576	4.20	3.51	1.000
16	34.75	50.0	1.000	2.68	3.51	0.763
17	39.71	50.0	1.000	4.72	3.51	1.000

18	63.20	50.0	0.704	3.26	3.51	0.927
19	24.50	50.0	1.000	3.18	3.51	0.907
20	36.70	50.0	1.000	3.54	3.51	1.000
21	62.00	50.0	0.724	3.20	3.51	0.910
22	16.04	50.0	1.000	3.24	3.51	0.922
23	19.45	50.0	1.000	3.72	3.51	1.000
24	34.09	50.0	1.000	4.17	3.51	1.000
25	20.46	50.0	1.000	2.48	3.51	0.706
26	23.83	50.0	1.000	4.41	3.51	1.000
27	77.54	50.0	0.518	4.12	3.51	1.000
28	35.68	50.0	1.000	4.58	3.51	1.000
29	45.30	50.0	1.000	2.84	3.51	0.810
30	54.13	50.0	0.888	4.12	3.51	1.000

The baseline fitting, neutral to the pollution, can be added to the provinces' scatterplot; therefore, the f_{PM} correction can be qualitatively evaluated as a contribution to reducing the noise of the data.

In Fig. 4 – left panel it can be appreciated how the correction, accounting for the effect of PM_{10} concentration, shifted the points near the interpolation curve, reducing the variance. As a measure of the error and of the model's goodness of fit RMSE (Root Mean Square Error), i.e. the square root of the mean squared distances between measurements and predictions of a model, was chosen. The contribution of the PM_{10} correction to the model can be measured by means of the RMSE between the prediction of the Enthalpy Method with and without the correction (Fig. 4 – right panel). The RMSE of the predictions with reference to the Enthalpy Method fitted on the neutral points is 0.221, while after the correction, the RMSE value is reduced to 0.149, showing a significant improvement of over 32.0%.

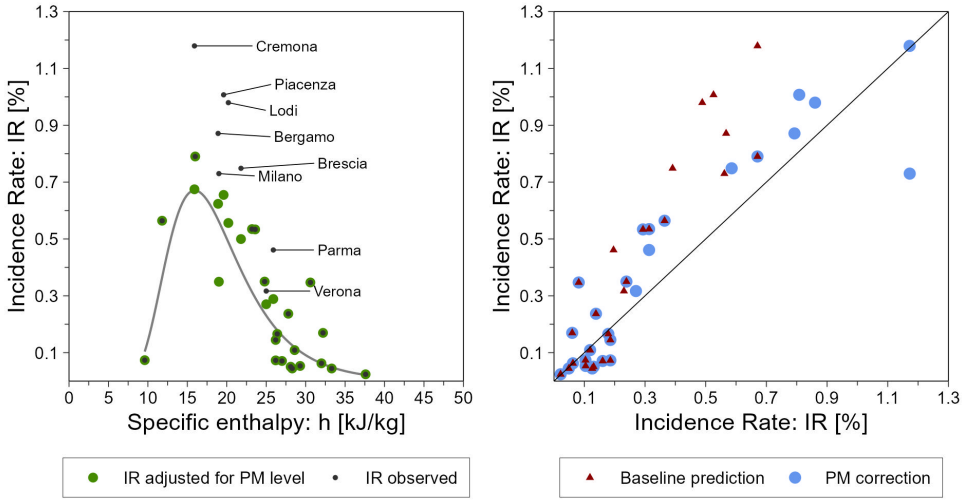

Fig. 4. left) Baseline interpolation curve of Incidence Rate (IR) vs. specific enthalpy (h) and scatterplot for the Italian Provinces listed in Table 2, with PM_{10} effect correction (green points) and without (black points); right) Scatterplot of the predicted Incidence Rate (IR) with and without PM_{10} effect correction. Predicted IR without f_{PM} correction (red) and corrected IR prediction (blue).

3.3 Ultraviolet Radiation Effect on Incidence Rate

The results of the calculations for the f_{UV} factor (as defined in §2.4) and the required data are listed in Table 2. The f_{UV} correction factor effect on the data can be observed in the following Fig. 5 – left panel, where the purple points (corrected) lie qualitatively closer to the baseline fit. As previously done in §3.1, the f_{UV} can be used to correct the predictions of the baseline Enthalpy Model (see Fig. 5 – right panel) and calculate the RMSEs in order to measure the improvement. The RMSE of the predictions concerning the enthalpy method fitted on the neutral points is 0.221, while after the correction is reduced to 0.179. This reduction shows a significant improvement of almost 19%, although minor with respect to the particulate matter correction.

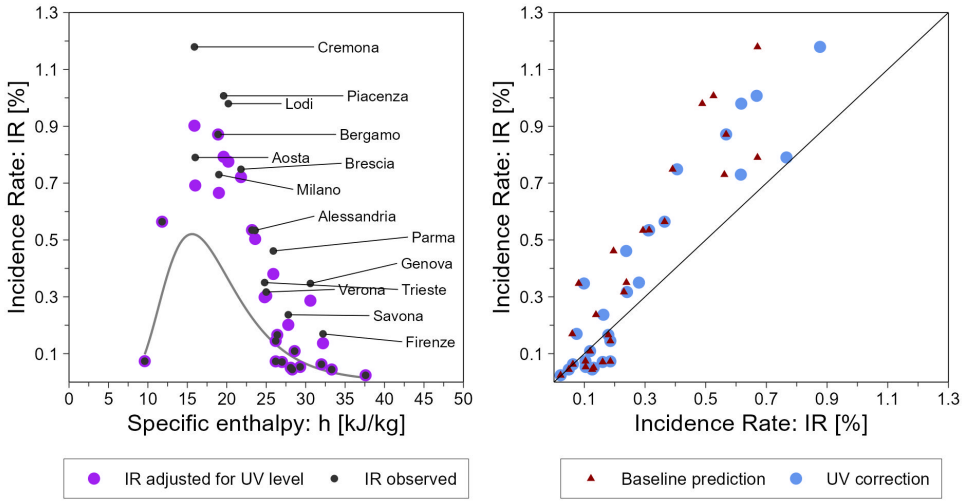

Fig. 5. left) Baseline interpolation curve of Incidence Rate (IR) vs. specific enthalpy (h) and scatterplot for the Italian provinces listed in Table 2, with UV effect correction (purple points) and without (black points); right) Scatterplot of the predicted Incidence Rate (IR) with and without UV effect correction. Predicted IR without f_{UV} correction (red) and corrected IR prediction (blue).

4 Discussion

4.1 Interaction Effects of PM and UV on Incidence Rate

In the following, Fig. 6 – left panel explores the interaction between the f_{UV} and f_{PM} correction factors on data. As can be observed, the red points (corrected) are qualitatively closer to the baseline fit. Continuing to use the RMSEs to evaluate and measure the ability of the corrections to improve the model, in Fig. 6 – right panel it can be seen the correction applied to the prediction of the baseline model. The RMSE of the predictions with reference to the Enthalpy Method fitted on the neutral points is again 0.221, while after the corrections, the RMSE value is reduced to 0.136, reaching a total improvement of over 38%.

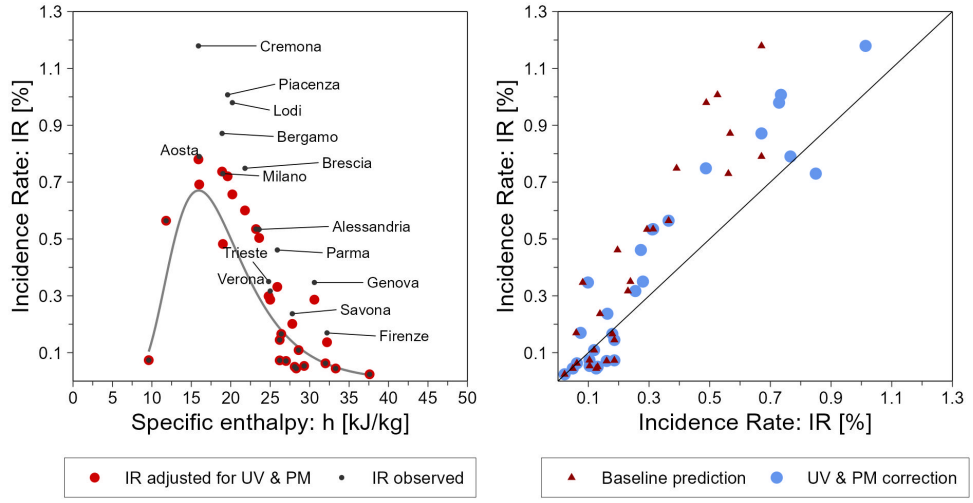

Fig. 6. left) Baseline interpolation curve of Incidence Rate (IR) vs. specific enthalpy (h) and scatterplot for the Italian provinces, with both PM_{10} and UV effects correction, namely f_{COR}, (red points) and without (black points); right) Scatterplot of the predicted Incidence Rate (IR) with and without PM_{10} and UV effects correction. Predicted IR without f_{COR} correction (red) and corrected IR prediction (blue).

4.2 Particulate Matter

The PM can act indifferently in outdoor and indoor environments as long as there is no filtering of the external air to address this pollutant, leading this environmental factor to interact with the host and the virions seamlessly. The findings clearly assess the role and the importance (higher than linear) of the PM in the dynamics of the disease's spread: the knowledge of the PM_{10} levels can improve (32% on RMSE basis) our ability to predict the incidence of the contagion in different locations, helping decision makers respond to the harm for the population.

4.3 Ultraviolet Radiation

The use of the DI irradiation level DI as a UV proxy is more challenging. The UV radiation acts on the host, intervening in vitamin D synthesis and benefiting the immune system. On the virus side, while the effectiveness of UV radiation in sterilisation processes is well known, it is based on UV-C frequencies and is conducted in controlled conditions. Only UV-A and UV-B frequencies of solar radiation are able to travel through the atmosphere, reaching the ground on Earth. Moreover, UV radiation acts in outdoor environments only, and the social habits of different community groups intervene in the probability of contagion as they spend more or less time outdoors. Based on relative levels, the correction factor f_{UV} can be applied only when data from the whole area considered are available so that it is possible to define the average level for the geographical area at hand.

4.4 Interaction Between PM and UV

Referring to our data, the overall correction based on the interaction between the two factors led to the best results, with an improvement in the RMSE of over 38%. However, the performance of the PM correction alone is not so far (32%) from the results of the overall

correction. In those terms, the influence of the two environmental conditions can be weighted, which steers us to conclude that PM levels reasonably play a more substantial role in the spread of the infection. This fact appears magnified by the fact that PM acts both in outdoor and indoor environments. As a matter of fact, the data on solar radiation are mainly available as average values with low time resolution (often just the mean value over a whole month); while the particulate matter data are more widely available due to the government's willingness to control the air quality. This fact could contribute to further explain the different effectiveness of the two correction factors (f_{PM} and f_{UV}).

4.5 Future Research

Provided that, among others, both the effectiveness of UV-A and UV-B – as present at ground level as a fraction of the solar radiation – in sterilising surfaces, and the risk of contagion through fomites in outdoor environments, could be better investigated, the exponent's values obtained for the corrective coefficients in this study should not be regarded as definitive estimates. Indeed, since these exponents were tailored to minimize errors based on the available data, a risk of overfitting exists, which could compromise the possibility of generalization to new datasets. This is the reason why the exact values of the exponents corresponding to the identified minimums were not employed; while, also considering the dataset's limited size, more reasonable and conservative values were proposed. Thus, future developments may include a reassessment of the corrective coefficients using larger datasets, which would enable a proper division into training and test sets. Additionally, further case studies could improve the applicability of the proposed methodology in different national or large community contexts.

Conclusions

The Enthalpy Method, recently introduced to predict the potential risk of coronavirus contagion in either outdoor and indoor environments, is basically founded on temperature and humidity patterns. Yet successfully tested for the SARS-CoV-2, it inherently does not consider the influence of other secondary weather agents. Indeed, the effect of particulate matter on the viability and spread of a virus is widely discussed by the scientific community nowadays. Moreover, the pollution acts also on the host, compromising the respiratory tract; while ultraviolet radiation is commonly recognised as a virus inhibitor.

In this frame, the aim of this study was to investigate the extent to which the major climatic confounding factors, namely pollution levels (here assumed in terms of PM_{10}) and solar direct irradiation levels DI (here assumed as a more readily available proxy for UV) can quantitatively influence the predictive outcomes not only of the Enthalpy Method, but in general of any infection spread model. The study revealed that the PM effects play the major confounding role (and this, regardless of its harmful activity both outdoor and indoor).

A PM correction factor was then first formulated to address the residual variance in the available data attributable to the increasing importance of this environmental parameter. It was demonstrated that adjusting the prediction for PM can reduce the noise of pandemic data, revealing a neater pattern in terms of Incidence Rate versus specific enthalpy estimations. Nonetheless, it was also possible to define a correction factor based on relative DI levels of a considered country, that led to further improved predictions (of almost 20% in terms of RMSE).

The two correction factors f_{PM} and f_{UV} have been successfully proven to be effective, at first individually, leading to better predictions in terms of Incidence Rate expectations. Anyway, whenever an interaction between PM and UV cannot be denied, it must be considered that their effects do not simply add up. Due to the fact that neglecting this

complexity can lead to oversized correction values, then a calibrated relationship to account for the interaction between f_{PM} and f_{UV} was also introduced. The need for further improvements was also addressed. Apart from the general opportunity that either the effectiveness of UV-A and UV-B – as a fraction of the solar radiation - in sterilising surfaces, either the risk of contagion through fomites in outdoor environments, may be better investigated, more specific future insights could include a reassessment of the corrective coefficients using larger datasets, which would enable a proper division into training and test sets. Additionally, further case studies could improve the applicability of the proposed methodology in different national or large community contexts.

Symbology

Symbol	
h	Specific enthalpy of a system, $kJ \cdot kg^{-1}$
c_a	Specific heat at the constant pressure of dry air, $kJ \cdot kg^{-1} \cdot °C^{-1}$
c_v	Specific heat at the constant pressure of water vapour, $kJ \cdot kg^{-1} \cdot °C^{-1}$
r	Latent heat of vaporization of water at its triple point, $kJ \cdot kg^{-1}$
t	Temperature of a system, °C
AH	Absolute humidity, ND
PM	Particulate matter
DI	Direct solar irradiation, $kWh \cdot m^{-2} \cdot day^{-1}$
IR	Incidence rate, %
f	Corrective factor, ND
UV	Ultraviolet radiation, ND
T_{PM10}	PM_{10} daily threshold, $\mu g \cdot m^{-3}$
C_{PM10}	average PM_{10} concentration recorded during the observation period, $\mu g \cdot m^{-3}$

References

1. N. van Doremalen, T. Bushmaker, D. H. Morris, M. G. Holbrook, A. Gamble, B. N. Williamson, A. Tamin, J. L. Harcourt, N. J. Thornburg, S. I. Gerber, J. O. Lloyd-Smith, E. de Wit, and V. J. Munster, Aerosol and surface stability of SARS-CoV-2 as compared with SARS-CoV-1. N. Engl. J. Med. **382**, 1564 (2020). https://doi.org/10.1056/NEJMC2004973
2. A. Spena, L. Palombi, M. Corcione, M. Carestia, and V. A. Spena, On the optimal indoor air conditions for SARS-CoV-2 inactivation. An enthalpy-based approach. Int. J. Environ. Res. Public Health. **17**, 6083 (2020). https://doi.org/10.3390/IJERPH17176083
3. A. Spena, L. Palombi, M. Corcione, A. Quintino, M. Carestia, and V. A. Spena, Predicting SARS-CoV-2 Weather-induced seasonal virulence from atmospheric air enthalpy. Int. J. Environ. Res. Public Health. **17**, 1 (2020). https://doi.org/10.3390/ijerph17239059
4. J. Cai, W. Sun, J. Huang, M. Gamber, J. Wu, and G. He, Indirect virus transmission in cluster of COVID-19 cases, Wenzhou, China, 2020. Emerg. Infect. Dis. **26**, 1343 (2020). https://doi.org/10.3201/EID2606.200412

5. E. Balboni, T. Filippini, K. J. Rothman, S. Costanzini, S. Bellino, P. Pezzotti, S. Brusaferro, F. Ferrari, N. Orsini, S. Teggi, and M. Vinceti, The influence of meteorological factors on COVID-19 spread in Italy during the first and second wave. Environ. Res. **228**, 115796 (2023). https://doi.org/10.1016/J.ENVRES.2023.115796
6. K. Demertzis, D. Tsiotas, and L. Magafas, Modeling and forecasting the COVID-19 temporal spread in Greece: An exploratory approach based on complex network defined splines. Int. J. Environ. Res. Public Health. **17**, 4693 (2020). https://doi.org/10.3390/IJERPH17134693
7. C. Magazzino, M. Mele, and N. Schneider, The relationship between air pollution and COVID-19-related deaths: An application to three French cities. Appl. Energy. **279**, 115835 (2020). https://doi.org/10.1016/J.APENERGY.2020.115835
8. D. Feurer, T. Riffe, M. S. Kniffka, E. Acosta, B. Armstrong, M. Mistry, R. Lowe, D. Royé, M. Hashizume, L. Madaniyazi, C. F. S. Ng, A. Tobias, C. Íñiguez, A. M. Vicedo-Cabrera, M. S. Ragettli, E. Lavigne, P. M. Correa, N. V. Ortega, J. Kyselý, A. Urban, H. Orru, E. Indermitte, M. Maasikmets, M. Dallavalle, A. Schneider, Y. Honda, B. Alahmad, A. Zanobetti, J. Schwartz, G. Carrasco, I. H. Holobâca, H. Kim, W. Lee, M. L. Bell, N. Scovronick, F. Acquaotta, M. de S. Z. S. Coélho, M. H. Diaz, E. E. F. Arellano, P. Michelozzi, M. Stafoggia, F. de'Donato, S. Rao, F. Di Ruscio, X. Seposo, Y. Guo, S. Tong, P. Masselot, A. Gasparrini, and F. Sera, Meteorological factors, population immunity, and COVID-19 incidence A global multi-city analysis. Environmental Epidemiology. **8**, e338 (2024). https://doi.org/10.1097/EE9.0000000000000338
9. L. Fedrizzi, M. Carugno, D. Consonni, A. Lombardi, A. Bandera, P. Bono, F. Ceriotti, A. Gori, and A. C. Pesatori, Air Pollution Exposure, SARS-CoV-2 infection, and immune response in a cohort of healthcare workers of a large university hospital in Milan, Italy. Environ. Res. **236**, 116755 (2023). https://doi.org/10.1016/J.ENVRES.2023.116755
10. A. Spena, L. Palombi, M. Carestia, V. A. Spena, and F. Biso, SARS-CoV-2 Survival on surfaces. Measurements optimisation for an enthalpy-based assessment of the risk. Int. J. Environ. Res. Public Health. **20**, 6169 (2023). https://doi.org/10.3390/IJERPH20126169
11. L. Setti, F. Passarini, G. de Gennaro, A. Di Gilio, J. Palmisani, P. Buono, G. Fornari, M. G. Perrone, A. Piazzalunga, P. Barbieri, E. Rizzo, and A. Miani, SIMA Position Paper: Relazione circa l'effetto dell'inquinamento da particolato atmosferico e la diffusione di virus nella popolazione (2020).
12. L. Setti, F. Passarini, G. De Gennaro, P. Barbieri, S. Licen, M. G. Perrone, A. Piazzalunga, M. Borelli, J. Palmisani, A. DI Gilio, E. Rizzo, A. Colao, P. Piscitelli, and A. Miani, Potential role of particulate matter in the spreading of COVID-19 in Northern Italy: first observational study based on initial epidemic diffusion. BMJ Open **10**, e039338 (2020). https://doi.org/10.1136/BMJOPEN-2020-039338
13. L. Setti, F. Passarini, G. De Gennaro, P. Barbieri, M. G. Perrone, M. Borelli, J. Palmisani, A. Di Gilio, V. Torboli, F. Fontana, L. Clemente, A. Pallavicini, M. Ruscio, P. Piscitelli, and A. Miani, SARS-Cov-2RNA found on particulate

matter of Bergamo in Northern Italy: First evidence. Environ. Res. **188**, 109754 (2020). https://doi.org/10.1016/J.ENVRES.2020.109754

14. P. Piscitelli, A. Miani, L. Setti, G. De Gennaro, X. Rodo, B. Artinano, E. Vara, L. Rancan, J. Arias, F. Passarini, P. Barbieri, A. Pallavicini, A. Parente, E. C. D'Oro, C. De Maio, F. Saladino, M. Borelli, E. Colicino, L. M. G. Gonçalves, G. Di Tanna, A. Colao, G. S. Leonardi, A. Baccarelli, F. Dominici, J. P. A. Ioannidis, and J. L. Domingo, The role of outdoor and indoor air quality in the spread of SARS-CoV-2: Overview and recommendations by the research group on COVID-19 and particulate matter (RESCOP commission). Environ. Res. **211**, 113038 (2022). https://doi.org/10.1016/J.ENVRES.2022.113038
15. D. Marín-Palma, G. J. Fernandez, J. Ruiz-Saenz, N. A. Taborda, M. T. Rugeles, and J. C. Hernandez, Particulate matter impairs immune system function by up-regulating inflammatory pathways and decreasing pathogen response gene expression. Scientific Reports. **13**, 1 (2023). https://doi.org/10.1038/s41598-023-39921-w

The views and opinions expressed in this article are solely those of the authors and do not reflect the official policy or position of any other organization.

The data supporting the findings of this study are included in the main text, tables, and figures of this article, or are freely available from the online public sources cited in the manuscript